Available online at www.sciencedirect.com
ScienceDirect
Journal of Power Sources 165 (2007) 224–231
JOURNAL OF POWER SOURCES
www.elsevier.com/locate/jpowsour

Modelling a PEM fuel cell stack with a nonlinear equivalent circuit

U. Reggiani, L. Sandrolini *, G.L. Giuliattini Burbui

Department of Electrical Engineering, Alma Mater Studiorum, University of Bologna, Viale del Risorgimento 2, I-40136 Bologna, Italy

Received 16 February 2006; received in revised form 20 June 2006; accepted 18 November 2006
Available online 16 January 2007

Abstract

A nonlinear circuit model of a polymer electrolyte membrane (PEM) fuel cell stack is presented. The model allows the simulation of both steady-state and dynamic behaviour of the stack on condition that the values of some of its parameters are changed in the two operating conditions. The circuit parameters can be obtained by means of simple experimental tests and calculations. A commercial PEM fuel cell stack is modelled as seen from the power conditioning system side, without requiring parameters necessary for complex mathematical models and not easily obtainable by the majority of users. A procedure of parameter determination is developed and a comparison between the simulated and experimental results for both steady-state and dynamic behaviour of the PEM stack is shown.

Keywords: Fuel cell; Polymer electrolyte membrane; Equivalent circuit; Voltage drop; Current interrupt method; Fitting

1. Introduction

Rising crude oil prices (with highs over US$ 70 a barrel during the last year) pose the exploitation of alternative energy sources as a serious challenge for the next future. Fuel cells appear one of the most appealing renewable energy technologies for their low environmental impact and high conversion efficiency. Their application ranges from stationary to portable power generation, including transportation. Modelling fuel cells is then necessary to simulate the behaviour of more complex systems (e.g., electric vehicles, or electric low-power plants or cogeneration systems), in which fuel cells are integrated as source of energy. Lots of papers present mathematical models for PEM fuel cells, in which their typical application requirements of high specific power, rapid start-up, low-temperature operation and ease of construction are met. Different load conditions, temperature and pressure of gases, as well as spatial dimensions of the cell [1], can thus be taken into account at the design level and simulation results can be of help in setting up operational strategies. Most of these models are however extremely complex, involving many partial differential equations and their boundary conditions, and need a lot of expertise in identifying and estimating their large number of parameters as detailed information on the cell is essential [2–4]. The variety of material properties to know, such as porosity, permeability, effective diffusion and charge transfer coefficients, makes these models cumbersome, and not often easily exploitable. Simplified models have also been proposed, in which the reversible voltage and the voltage drops are summarized in simpler equations [5–7]. On the other hand, complex mathematical models can be simplified with the introduction of some empirical equations instead of partial differential equations [8,9]. These equations use fitting coefficients obtained from experimental data and are therefore related to a particular operating condition. This means that the equations may fail to predict experimental data in different conditions. The steady-state performance of a fuel cell stack can be represented by the majority of these models, resulting in the so called polarisation curve, that is a plot of voltage versus current density for a given set of operating conditions. Besides, the dynamic behaviour of a fuel cell stack cannot be disregarded in all those applications where mechanical, thermal or electrical quantities have fast variations [9,10]. Commercial fuel cell systems are power modules that include also auxiliary circuitry to control subsystems for fuel and air supply, and water disposal. This paper will be focused to model a commercial fuel cell stack as seen from the power conditioning system

* Corresponding author. Tel.: +39 051 2093484; fax: +39 051 2093588.
E-mail addresses: ugo.reggiani@mail.ing.unibo.it (U. Reggiani), leonardo.sandrolini@mail.ing.unibo.it (L. Sandrolini), gianlorenzo.giuliattini@mail.ing.unibo.it (G.L. Giuliattini Burbui).

0378-7753/$ – see front matter © 2006 Elsevier B.V. All rights reserved.
doi:10.1016/j.jpowsour.2006.11.062

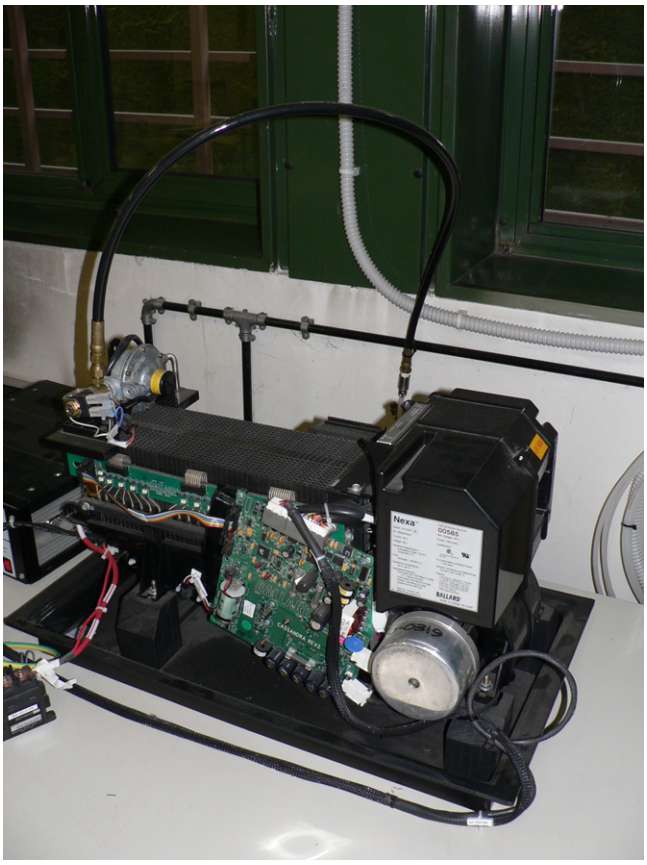

Fig. 1. Fuel cell stack used in the experiments.

side, i.e., electronic converters which interface such source to the electrical grid and/or the load, without requiring parameters either not easily obtainable by the majority of users or confidential to the manufacturers only. The model represents the overall system, i.e., fuel cell stack and auxiliary circuitry, as shown in Fig. 1. The performance of the stack is suitably described with a simple circuit model that can be represented in terms of an equivalent circuit. The model allows the simulation of both steady-state and dynamic behaviour of the stack. With reference to other circuit models of PEM fuel cells that have been recently presented in the literature [11–15], the parameters of the proposed model can be determined through simple experiments and calculations which still offer insight into the nonlinear phenomena occurring in a fuel cell. Moreover, the model is applicable to PEM fuel cells that lack detailed information. A comparison between experimental and numerical results obtained with the model presented in this paper is made and discussed.

2. Basic operating principles of a PEM fuel cell

A PEM fuel cell consists of two electrodes separated by a thin layer of catalyst in contact with a plastic permeable membrane that allows protons to pass through but prohibits the passage of reactant gases. The electrodes and the membrane are pressed between two conductive plates containing some channels through which the gases (hydrogen and oxygen) are fed from gas supply chambers. The electrodes and the membrane, which acts as an electrolyte, form a structure with an overall thickness of less than a millimeter. The electrodes have a porous structure which allows the reactants to flow. The chemical reactions that occur at the catalyst layer yield hydrogen ions and electrons at the anode

$$H_2 \rightarrow 2H^+ + 2e^-, \tag{1}$$

and water (and heat energy as a by-product) at the cathode

$$\tfrac{1}{2}O_2 + 2H^+ + 2e^- \rightarrow H_2O. \tag{2}$$

The hydrogen ions cross the membrane, while the electrons flow through the external circuit connected to the electrodes generating useful current. To achieve the power and voltage required by the system connected to the fuel cell, several single cells can be connected in series into a fuel cell stack.

3. Circuit models

Irreversible losses that occur under operating conditions make the voltage of a fuel cell stack less than its reversible value, V_{rev}. This is the theoretical value of the open-circuit voltage, and for a hydrogen fuel cell stack it is given by the formula [5]

$$V_{rev} = -N_{cell}\frac{\Delta \bar{g}_f}{2F}, \tag{3}$$

where $\bar{g}_f$ is the molar Gibbs free energy, F the Faraday constant and N_{cell} is the stack fuel cell number. A simple analytical model can be based on the main voltage drops only, i.e., the activation voltage drop V_{act}, the ohmic voltage drop V_{ohm}, and the concentration voltage drop V_{conc}. Voltage drops in a fuel cell can also occur either for cathode flooding, when the water produced by the chemical reaction is not effectively removed [10], or for membrane dehydration. In many fuel cell models the membrane is considered as being completely saturated of water [9] and therefore hydration issues of the membrane are neglected. Besides, when all the variables that govern the rate of water formation (i.e., the current) or removal (i.e., the temperature and pressure) are kept in the range prescribed by the cell manufacturer, also the voltage drops due to cathode flooding may be ignored. Other causes of voltage drop are related to the diffusion of some hydrogen molecules and of some electrons to the cathode through the membrane. The former phenomenon, known as fuel crossover, is more important, and represents a waste of fuel. Both phenomena are basically equivalent, as they result in two electrons per hydrogen molecule that go from the anode to cathode internally rather than through the external circuit, and can be referred to as an internal current. Although the amount of electrons is small, it does cause a sensible voltage drop at open-circuit, especially with low-temperature cells, such as PEM ones [5]. As this voltage drop is particularly significant for small currents, it can be comprised in the activation voltage drop. The total stack voltage, V_T, is then obtained excluding all the voltage drops from the reversible voltage

$$V_T = V_{rev} - V_{act} - V_{ohm} - V_{conc}. \tag{4}$$

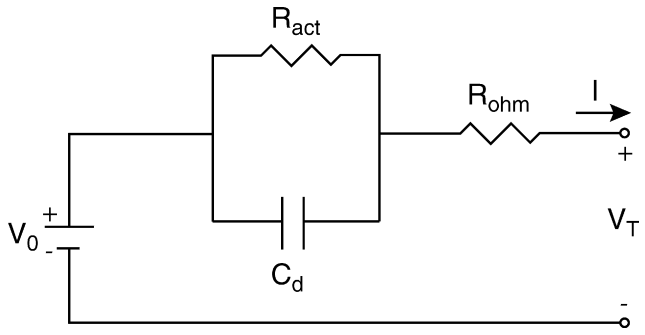

Fig. 2. Equivalent circuit of a PEM fuel cell stack.

The dynamic behaviour of a PEM fuel cell stack can be represented by means of a simple first-order equivalent circuit such as the one depicted in Fig. 2 [5,7,16]. The ohmic voltage drop is represented through the resistor R_{ohm}, which expresses the internal resistance of the cell stack, i.e., the resistance due to nonideal electrodes and conductive plates and to proton transfer through the membrane [5,9]. The activation voltage drop is represented through the parallel connection of a resistor, R_{act}, with a capacitor, C_d, that models the double layer of charge at the interfaces between the membrane and the electrodes. The dc voltage source V_0 is the effective open-circuit voltage of the fuel cell stack. The model does not provide for the concentration voltage drop, related to changes in the concentration of oxygen and hydrogen at the electrodes due to the continuous chemical reaction. Although in a well designed system with good oxygen and hydrogen supplies this drop should be very small at the rated current [5], it may be taken into account by an impedance in series with R_{act}. As the elements of this simple circuit are assumed linear, the simulation of complex nonlinear phenomena such as the ones occurring in a fuel cell stack is not always appropriate. In particular, neither the internal current effect, nor currents greater than the rated one can be treated with this model. Furthermore, at steady-state the equivalent circuit of Fig. 2 is reduced to a resistive circuit and, consequently, the voltage drops at steady-state are simply proportional to the current supplied. The voltage versus current density curve of the fuel cell stack would therefore result in a linear steady-state performance curve, that approximates the experimental performance curve just for intermediate current density values, but not for low or high current density values. The aim of this paper is to present an equivalent circuit able to approximate both dynamic and steady-state behaviour of the stack.

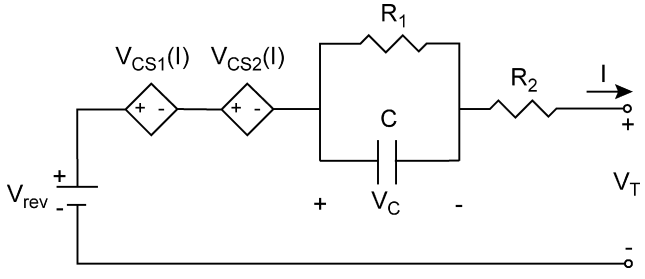

Fig. 3. Proposed equivalent circuit.

4. Proposed model

In order to simulate the cell stack behaviour effectively, in particular in steady-state conditions, a more complex circuit model is developed, with nonlinear active and passive components. With reference to Fig. 3, the circuit contains two nonlinear current controlled voltage sources $V_{CS1}(I)$ and $V_{CS2}(I)$, which can be related to the activation and concentration voltage drops, respectively. As it is known, these voltage drops can be expressed as

$$V_{act} = f_1(I) = A_{stack} \ln\left(\frac{I + I_n}{I_0}\right), \tag{5}$$

and

$$V_{conc} = f_2(I) = -B \ln\left(1 - \frac{I}{I_L}\right). \tag{6}$$

In (5) A_{stack} is Tafel's stack coefficient; I, I_n and I_0 are the output, internal and exchange currents of the stack, respectively. In (6) B is an empirical coefficient and I_L is the limiting current. It can be assumed that $V_{CS2} = f_2(I)$.

With respect to the model proposed in [14], the developed model considers the effect of the internal current on the activation drop and takes the influence of the temperature on the reversible voltage into account [2,6], being

$$V_{rev} = N_{cell}\left[1.23 - 0.9 \times 10^{-3}(T - 298) + \frac{RT}{2F} \ln\left(\frac{p_{H_2} p_{O_2}^{1/2}}{p_{H_2O}}\right)\right], \tag{7}$$

where R is the universal gas constant, T the operating absolute temperature and p is the partial pressure of the different species. Constant pressures of gases are assumed to simplify the model.

In regard to the passive elements of the equivalent circuit shown in Fig. 3, the capacitor C affects the transient behaviour whereas the meaning of the resistors R_1 and R_2 is highlighted in the next section.

5. Experimental

The analysis of the steady-state and dynamic behaviour of the model is made by comparing simulated and measured results. The experimental tests were carried out on a commercial PEM fuel cell system composed of a cell stack and auxiliary circuitry for internal regulation. The stack was a series of 47 membrane electrode assemblies (MEAs) comprising a Nafion 112 membrane with a thickness of 50 μm. The active area of the electrodes was 115.8 cm^2. The system had a rated output power of 1.2 kW at a voltage of 26 V and the open-circuit voltage was 43 V. The auxiliary circuitry shuts down the fuel cell stack when the stack current reaches the rated current value.

The electrochemical impedance spectroscopy (EIS) is a widely accepted method for parameter determination of PEM fuel cell stack equivalent circuits. In this tests small signals of variable frequency alternating current are superimposed to

a steady-state operating point of the cell stack. The fuel cell stack impedance spectrum is obtained from the measured voltage across the stack, and the parameter values of the adopted equivalent circuit can be determined using a fitting procedure. Nevertheless, this method cannot be applied to equivalent circuits with active elements, such as controlled sources. In this case, the current interrupt method (CI) is well suitable [5,16–19]. When the current of the cell stack is interrupted, the stack voltage has an instantaneous rise, ΔV_{ohm}, equal to the ohmic voltage drop, and then it moves to the open-circuit voltage value, V_0, with an increase, ΔV_{act}, that equals the change of the activation voltage drop, provided that the operating current is low enough so that the concentration voltage drop is negligible. However, it may often result very difficult to accurately carry out the graphical estimates of the voltage rise, which make the method so simple in principle. In fact, the point where the vertical transition ends may not be exactly discriminated, yielding a possible overestimate of the ohmic voltage rise. Another difficulty in interpreting the results is introduced by real oscilloscopes, which do not show the vertical voltage rise ideally expected. However, these limitations can be overcome by extrapolating the transient voltage curve at the moment of the current interruption with an appropriate time scale [16,20–22]. In this way, the ohmic contribution, ΔV_{ohm}, to the voltage rise of the stack can be separated from that related to the activation phenomena, ΔV_{act}. Several CI tests were performed at different operating conditions, which can be varied by connecting the fuel cell to a home-built electronic load, depicted in Fig. 4. Eight modules, each composed of power resistors and a N-type MOSFET transistor, dissipating a maximum power of 150 W, are connected in parallel. A time range of 100 μs was chosen to separate the ohmic voltage rise contribution from the activation one (see Fig. 5) through the extrapolation procedure. Although voltage spikes preceding and following the interruption, due to the feedback control of the electronic load, can be noticed, they do not affect the estimate of the ohmic voltage rise.

Voltage transients following the instantaneous ohmic voltage rise during CI tests were measured. The whole test set-up, comprising the PEM fuel cell stack and the electronic load, is shown in Fig. 6.

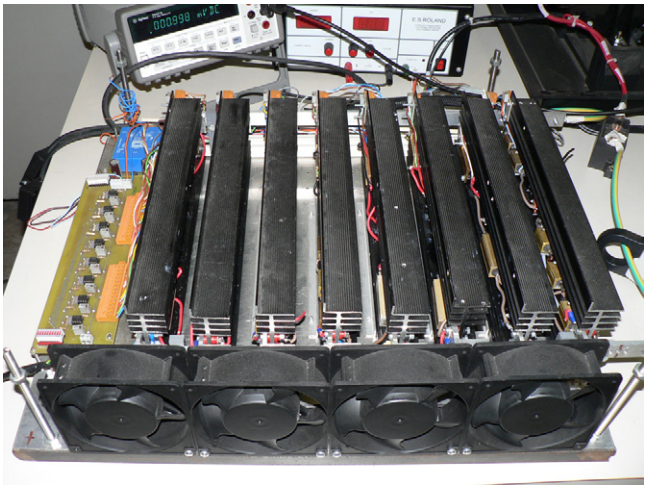

Fig. 4. Home-built electronic load used in the CI tests.

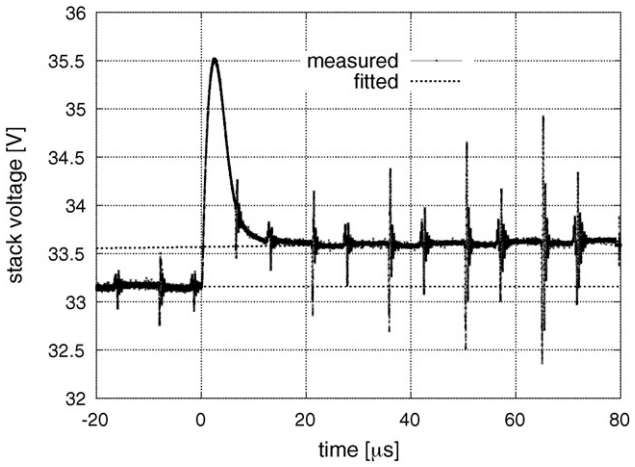

Fig. 5. Voltage transient (solid line) and fitted voltage (dashed line) following a 10.04 A current interruption.

Fig. 6. Test set-up used in the CI tests.

The experimental tests were completed with the measurement of the steady-state stack voltage versus current characteristic. The stack temperature varied between 25 and 65 °C.

6. Results and discussion

The results of the CI tests are summarized in Table 1. For each value of the operating current I the ohmic resistance is evaluated

Table 1
PEMFC CI test results

Test	I (A)	ΔV_{ohm} (V)	R_{ohm} (Ω)
1	4.4	0.14	0.031
2	6.2	0.25	0.040
3	8.2	0.32	0.040
4	10.0	0.43	0.043
5	12.2	0.49	0.040
6	14.3	0.58	0.041
7	16.2	0.66	0.041

from the determined ohmic voltage rise, ΔV_{ohm}, as

$$R_{ohm} = \frac{\Delta V_{ohm}}{I}. \quad (8)$$

The value of the ohmic resistance of the PEM fuel cell system varied from 31 to 43 mΩ in the tests. An average value of 39 mΩ (standard deviation $\sigma = 4$ mΩ) was then chosen for the resistor R_{ohm}. This value corresponds to an areal resistance of 0.096 Ω cm^2 and a resistivity in the normal direction of 19.22 Ω cm which are consistent with published data [23–27]. However, it is difficult to make comparisons as the measurement techniques are different and the tests are carried out on a single cell or an isolated membrane in some cases and on a whole stack in others. With respect to [28], the lower resistance value found in this paper can be related to the shorter overshoot produced by the improved load. The absence of inductive oscillations allowed the ohmic voltage rise to be determined with higher accuracy.

Recalling (5), the activation voltage rise ΔV_{act} that occurs during the CI transient can be written as

$$\Delta V_{act} = f_1(I) - f_1(0). \quad (9)$$

It was chosen not to estimate ΔV_{act} from a transient output voltage as the remaining contribution to the voltage rise. In fact, a steady-state condition could not be necessarily reached by the fuel cell module even with a longer transient time range. The quantity ΔV_{act} is evaluated through the experimental steady-state stack voltage versus current characteristic. In fact, as at low currents the activation loss is almost entirely responsible for the stack voltage drop [2,6], the initial trait of the experimental steady-state stack voltage versus current characteristic can be used to approximate the activation voltage drop $f_1(I)$, provided that the ohmic voltage drop is taken into account. These $f_1(I)$ experimental values allow the activation voltage drop versus current curve to be built in the operating current range of the PEM stack. The least-squares method used to fit (5) to these experimental values yielded $A_{stack} = 3.0 \pm 0.1$ V, $I_n = 0.6 \pm 0.1$ A, $I_0 = 5 \pm 1$ mA. These values correspond to the Tafel's cell coefficient $A_{cell} = 63.8$ mV and to the current densities $J_n = 5.2$ mA cm^{-2} and $J_0 = 0.04$ mA cm^{-2}, which are in the range of values reported in literature [5,29–32]. The activation voltage drop $f_1(I)$ is shown in Fig. 7. From Fig. 7 $\Delta V_{act} = f_1(I) - f_1(0)$ is obtained.

The dynamic behaviour of the proposed equivalent circuit is examined when disconnecting a load. With reference to Fig. 8, the time constant τ of the R_1C parallel can be evaluated through a fitting procedure of the voltage transient following the instantaneous ohmic voltage rise during a CI test with a time range of 5 s. At the moment of the load current interruption, the voltage across the R_1C parallel is equal to ΔV_{act}. In fact, at the end of the voltage transient following the instantaneous ohmic voltage rise, the stack voltage rise is equal to ΔV_{act} and in the proposed equivalent circuit this voltage rise is due to the capacitor discharge through R_1. As the voltage across a capacitor is continuous in time, the voltage across R_1 is ΔV_{act} also at the moment immediately preceding the load current interruption, when the steady-state current I flows through R_1. Consequently,

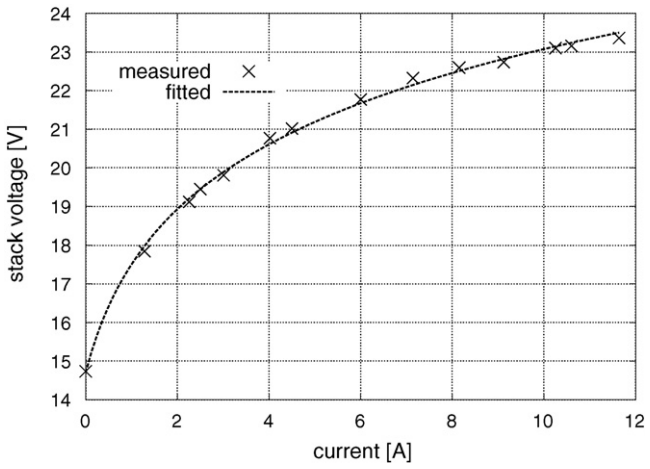

Fig. 7. Activation voltage drop vs. current curve for the PEM fuel cell stack.

R_1 can be calculated as

$$R_1(I) = \frac{\Delta V_{act}}{I} = \frac{f_1(I) - f_1(0)}{I}. \quad (10)$$

Being $\tau = R_1C$, the capacitance C can be obtained at the different operating currents. Fig. 9 shows the capacitance values obtained with the voltage transient fitting procedure and the analytical fitting curve

$$C(I) = a \ln\left(\frac{I}{I_{ref}}\right) + b, \quad (11)$$

where I_{ref} is a unitary reference current, $a = 0.034 \pm 0.001$ mF and $b = 0.040 \pm 0.003$ mF. During the transient following the instantaneous ohmic voltage rise (4) reduces to

$$V_T = V_{rev} - V_{act} \quad (12)$$

being $V_{ohm} = 0$. Moreover, as the concentration voltage drop is usually negligible for currents lower than the rated one and it is difficult to take it into account dynamically, the current controlled voltage source V_{CS2} is neglected. In the equivalent circuit of Fig. 3 this transient is represented by the capacitor discharge

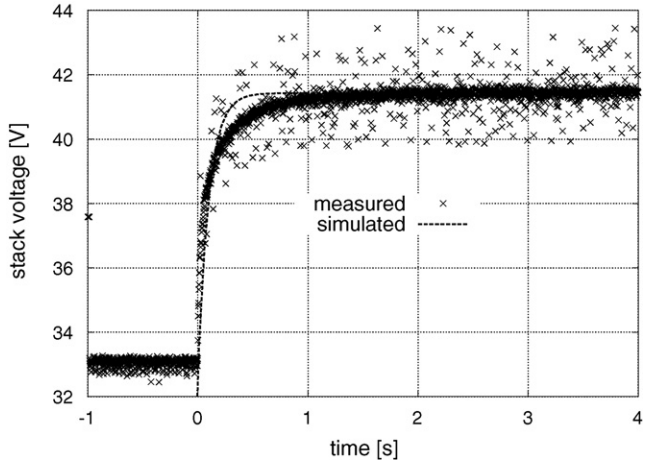

Fig. 8. Measured and simulated stack voltage transient following a 10.04 A current interruption.

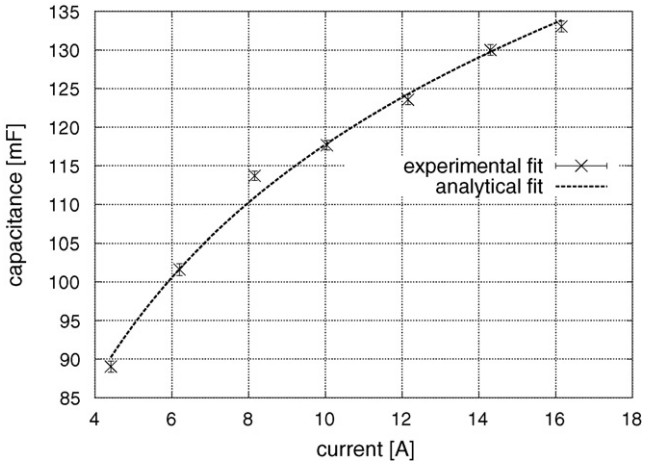

Fig. 9. Capacitance values for the proposed equivalent circuit.

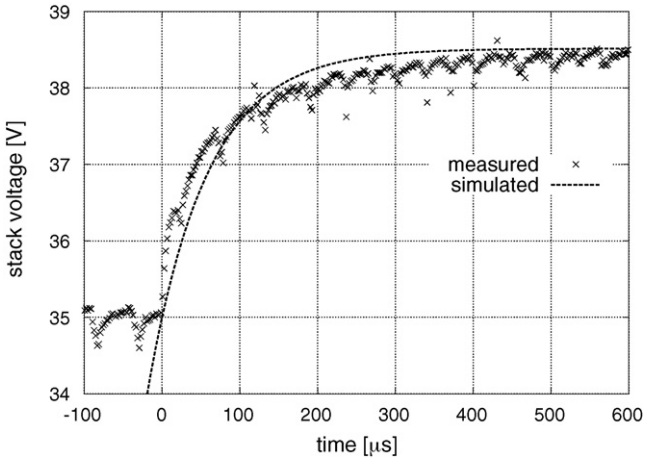

Fig. 10. Measured and simulated stack voltage transient for a current variation from 6.10 to 2.39 A.

through the resistor R_1 and the Kirchhoff's voltage law yields to

$$V_T = V_{rev} - V_{CS1} - V_C, \tag{13}$$

where

$$V_C = [f_1(I) - f_1(0)]\, e^{-t/R_1 C}. \tag{14}$$

From (12)–(14) it follows that during this transient the following equation holds

$$V_{act} = V_{CS1} + [f_1(I) - f_1(0)]\, e^{-t/R_1 C}. \tag{15}$$

It is easy to verify that the value of the current controlled voltage source V_{CS1} to be considered in order to satisfy the boundary conditions of the transient is $V_{CS1} = f_1(0)$. In fact, the value of V_{act} at the moment immediately preceding the interruption of the load current (time $t = 0$) is then $f_1(I)$, and the value of V_{act} at the end of the capacitor discharge ($t \to \infty$, no-load steady-state behaviour) is $f_1(0)$. It can be noticed that at this last operating condition $V_T = V_0$ and thus from (5) and (12) it follows

$$f_1(0) = A_{stack} \ln\left(\frac{I_n}{I_0}\right) = V_{rev} - V_0. \tag{16}$$

As Fig. 8 shows, a good agreement between the measured stack voltage transient and that simulated with the proposed circuit is obtained. For transients different than the one examined, where the load current varies suddenly from I_1 to I_2 steady-state values, the above considerations still hold, provided that currents I and 0 are replaced by I_1 and I_2, respectively. It follows that for a given transient the resistor R_1 depends on both bound state currents of the transient. The simulation for a stack voltage transient in which the current decreases from 6.10 to 2.39 A is plotted with the experimental result in Fig. 10. The results are still in good agreement also for larger current variations, as shown in Fig. 11, where the transient following the current variation between 19.99 and 12.03 A is depicted.

At a steady-state operating condition the voltage across the capacitor (14) is equal to zero but the capacitor behaves as an open-circuit. These two conditions can be satisfied simultaneously only if at steady-state the value of R_1 equals zero. From the circuit of Fig. 3 we have

$$V_T = V_{rev} - V_{CS1} - R_2 I, \tag{17}$$

where I denotes a steady-state current. Introducing the expressions of V_{act} and V_{ohm} into (4) we can write

$$V_T = V_{rev} - f_1(I) - R_{ohm} I. \tag{18}$$

Eqs. (18) and (17) yield $R_2 = R_{ohm}$ and the steady-state value $V_{CS1} = f_1(I)$. In Fig. 12, good agreement can be noticed between the measured and calculated steady-state stack voltage versus current characteristics. The concentration voltage drop was not taken into account in the calculation, as the limiting current I_L was not known. This drop occurs at very high current densities, which could not be anyway reached by the fuel cell stack under test, as the maximum operating current value was purposely limited by the constructor. It can be noticed that the controlled source V_{CS1} gives the activation voltage drop $V_{act} = f_1(I)$, being I the current at a steady-state operating condition or the steady-state current at the end of a transient. The resistor R_1 has a

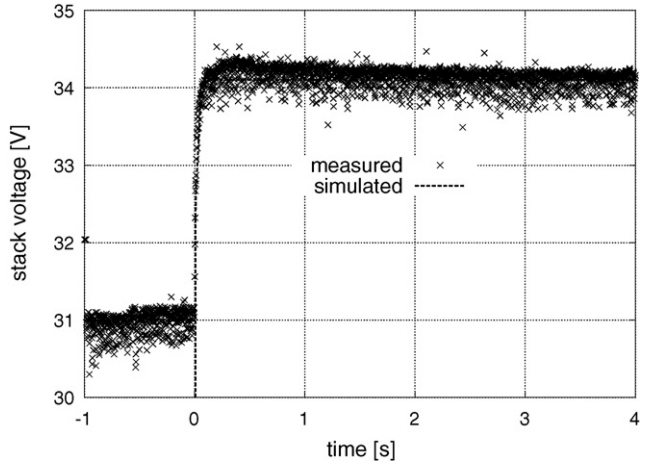

Fig. 11. Measured and simulated stack voltage transient for a current variation from 19.99 to 12.03 A.

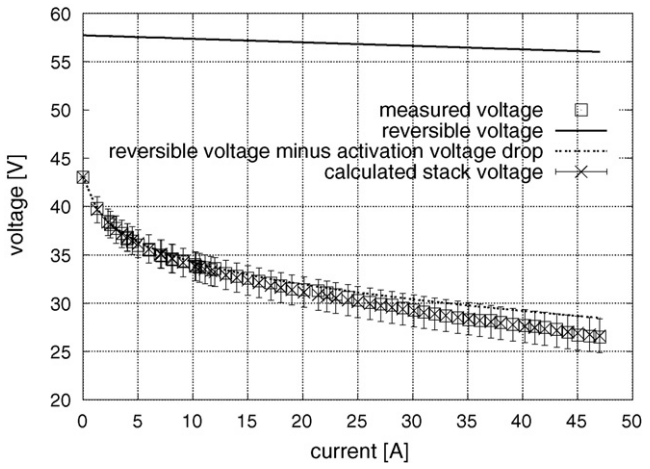

Fig. 12. Measured stack voltage and voltage drops implemented in the model vs. current in steady-state conditions.

resistance equal to zero at steady-state and is a nonlinear parameter depending on the current during a transient. Consequently, the capacitor C connected in parallel with R_1 is also a nonlinear current-dependent parameter. The dependence of the resistance $R_{ohm} = R_2$ on the current may be neglected choosing its average value in the considered operating current range of the PEM stack.

It has to be highlighted that the aim of this paper is mainly to present a model for a commercial PEM cell stack supplying the electrical grid and/or a load through the interfacing with electronic power converters. The objective is to have at one's disposal a model for the whole complex power electrical system of which the fuel cell stack is part. As a consequence, the proposed model has been validated in the operating range of a commercial fuel cell stack whose auxiliary circuitry does not allow currents higher than the rated one to be obtained. However, it can reasonably be expected that the proposed model is suitable to take account of the concentration voltage drops, too. In fact, the stack voltage versus current characteristic could be experimentally measured in a stack where the auxiliary circuitry can be deactivated. If the limiting current is known from the cell manufacturer, the model with the controlled source V_{CS2} can be fitted to the experimental results in order to find the empirical coefficient B. The comparison between measured and calculated voltage versus current characteristics allows the model to be validated.

7. Conclusions

A circuit model for a PEM fuel cell stack is presented. The model is nonlinear and can be used to simulate the steady-state and dynamic behaviour of the PEM stack if the values of some of its parameters are changed in the two operating conditions. The circuit parameter values are determined through simple experimental tests and calculations. A good agreement between the simulated and experimental results for both steady-state and dynamic behaviour of the PEM stack is obtained.

Acknowledgements

This work was supported in part under grant 200209 8425_002 of the Italian Ministry for University and Research.

The authors are grateful to Mr. Andrea Albertini for the valuable support given in designing and building the electronic load used in the experiments.

References

[1] T.E. Springer, T.A. Zawodzinski, S. Gottesfeld, J. Electrochem. Soc. 138 (8) (1991) 2334–2342.
[2] D.M. Bernardi, M.W. Verbrugge, J. Electrochem. Soc. 139 (9) (1992) 2477–2491.
[3] A. Rowe, X. Li, J. Power Sources 102 (2001) 82–96.
[4] L. Pisani, G. Murgia, M. Valentini, B. D'Aguanno, J. Power Sources 108 (2002) 192–203.
[5] J.E. Larminie, A. Dicks, Fuel Cell System Explained, second ed., John Wiley & Sons, Chichester, United Kingdom, 2000.
[6] G. Maggio, V. Recupero, L. Pino, J. Power Sources 101 (2001) 275–286.
[7] A.R. Balkin, Modelling a 500 W polymer electrolyte membrane fuel cell, Master's Thesis, University of Technology, Sydney, Australia, 2002.
[8] L. Pisani, G. Murgia, M. Valentini, B. D'Aguanno, J. Electrochem. Soc. 149 (7) (2002) A898–A904.
[9] M. Ceraolo, C. Miulli, A. Pozio, J. Power Sources 113 (2003) 131–144.
[10] S. Yerramalla, A. Davari, A. Feliachi, J. Power Sources 124 (2003) 104–113.
[11] C. Wang, M.H. Nehrir, S.R. Shaw, IEEE Trans. Energy Convers. 20 (2) (2005) 442–451.
[12] D. Yu, S. Yuvarajan, 19th Annual IEEE Applied Power Electronics Conference and Exposition—APEC 2004, Anaheim, CA, United States, 2004, pp. 362–366.
[13] A.M. Azmy, I. Erlich, Proc. 2003 IEEE Bologna Power-Tech. Conf., Bologna, Italy, 2003, pp. 1–6.
[14] P. Famouri, R.S. Gemmen, Proc. 2003 IEEE Power Eng. Soc. General Meeting, Toronto, Canada, 2003, pp. 1436–1440.
[15] Y.H. Kim, S.S. Kim, IEEE Trans. Energy Convers. 14 (2) (1999) 239–244.
[16] C.G. Lee, H. Nakano, T. Nishina, I. Uchida, S. Kuroe, J. Electrochem. Soc. 145 (8) (1998) 2747–2751.
[17] T. Abe, H. Shima, K. Watanabe, Y. Ito, J. Electrochem. Soc. 151 (1) (2004) A101–A105.
[18] J. Garnier, M.C. Pera, D. Hissel, F. Harel, D. Candusso, N. Glandut, J.P. Diard, A. De Bernardinis, J.M. Kauffmann, G. Coquery, 03 IEEE 58th Vehicular Technology Conference, VTC2003-Fall, vol. 58, Orlando, FL, United States, 2004, pp. 3284–3288.
[19] W. Choi, P.N. Enjeti, J.W. Howze, 19th Annual IEEE Applied Power Electronics Conference and Exposition—APEC 2004, Anaheim, CA, United States, 2004, pp. 355–361.
[20] F.N. Büchi, A. Marek, G.G. Scherer, J. Electrochem. Soc. 142 (6) (1995) 1895–1901.
[21] T.R. Ralph, G.A. Hards, J.E. Keating, S.A. Campbell, D.P. Wilkinson, M. Davis, J. St-Pierre, M.C. Johnson, J. Electrochem. Soc. 144 (11) (1997) 3845–3857.
[22] T. Mennola, M. Mikkola, M. Noponen, T. Hottinen, P. Lund, J. Power Sources 112 (2002) 261–272.
[23] K.M. Nouel, P.S. Fedkiw, Electrochim. Acta 43 (16–17) (1998) 2381–2387.
[24] F. Büchi, G. Scherer, J. Electrochem. Soc. 148 (3) (2001) 183–188.
[25] R. Silva, M. De Francesco, A. Pozio, J. Power Sources 134 (2004) 18–26.
[26] Y. Song, J.M. Fenton, H.R. Kunz, L.J. Bonville, M.V. Williams, J. Electrochem. Soc. 152 (3) (2005) 539–544.

[27] M. Tsampas, A. Pikos, S. Brosda, A. Katsaounis, C. Vayenas, Electrochim. Acta 51 (13) (2006) 2743–2755.
[28] U. Reggiani, L. Sandrolini, G.L. Giuliattini Burbui, A. Melotti, A. Massarini, Proc. Power Electronics Technology Exhibition and Conference, 2004, Chicago, USA, 2004, pp. 1–10.
[29] D. Chu, R. Jiang, J. Power Sources 80 (1–2) (1999) 226–234.
[30] S. Giddey, F.T. Ciacchi, S.P.S. Badwal, J. Power Sources 125 (2004) 155–165.
[31] W. Friede, S. Raël, B. Davat, IEEE Trans. Power Electron. 19 (5) (2004) 1234–1241.
[32] J. Stumper, H. Haas, A. Granados, J. Electrochem. Soc. 152 (4) (2005) A837–A844.